nature structural & molecular biology

Redox regulation of OxyR requires specific disulfide bond formation involving a rapid kinetic reaction path

Cheolju Lee[1,3], Soon Mi Lee[1], Partha Mukhopadhyay[5], Seung Jun Kim[1,2], Sang Chul Lee[2], Woo-Sung Ahn[3], Myeong-Hee Yu[4], Gisela Storz[5] & Seong Eon Ryu[1,2]

The *Escherichia coli* OxyR transcription factor is activated by cellular hydrogen peroxide through the oxidation of reactive cysteines. Although there is substantial evidence for specific disulfide bond formation in the oxidative activation of OxyR, the presence of the disulfide bond has remained controversial. By mass spectrometry analyses and *in vivo* labeling assays we found that oxidation of OxyR results in the formation of a specific disulfide bond between Cys199 and Cys208 in the wild-type protein. In addition, using time-resolved kinetic analyses, we determined that OxyR activation occurs at a rate of 9.7 s^{-1}. The disulfide bond–mediated conformation switch results in a metastable form that is locally strained by ~3 kcal mol^{-1}. On the basis of these observations we conclude that OxyR activation requires specific disulfide bond formation and that the rapid kinetic reaction path and conformation strain, respectively, drive the oxidation and reduction of OxyR.

Cellular reactive oxygen species (ROS) are generated as byproducts of oxygen respiration and as second messengers in cellular signaling[1,2]. ROS are capable of oxidizing many cellular components including DNA, lipid membranes and proteins, resulting in damage to cells. To avoid the harmful effects of ROS, cells have evolved mechanisms to respond to the oxidative damage. The *E. coli* OxyR transcription factor effectively senses low amounts of intracellular hydrogen peroxide (H_2O_2) and elicits the transcription of antioxidant genes[3,4]. In addition to H_2O_2, other oxidizing agents such as nitric oxide (NO) also have been implicated in regulating OxyR function[5]. Oxidation of OxyR induces a change in DNA-binding specificity and recruitment of RNA polymerase, leading to the induction of target genes[6–8].

The activation of OxyR begins with oxidation of the reactive Cys199 residue[4,9,10]. However, the subsequent activation mechanism is not fully understood yet. Various studies have concluded that OxyR activation involves formation of an intramolecular disulfide bond between Cys199 and Cys208 (refs. 4,9,10). The Cys199-Cys208 disulfide bond also was seen in the crystal structure of oxidized OxyR[11]. Nevertheless, the role of the Cys199-Cys208 disulfide bond has recently been questioned based on a study that could not detect the bond in air-oxidized OxyR[12]. This study also found that Cys199 is modified to S-NO, S-OH and S-SG upon exposure to different oxidizing and nitrosylating agents, which result in different OxyR responses.

The crystal structure of OxyR in reduced form reveals that Cys199 and Cys208 are separated by 17 Å, which is too far for disulfide bond formation[11]. Despite the large separation, the structure of the oxidized form reveals a disulfide bond between the two cysteines, which is associated with a large structural change within the regulatory domain. This structural change affects the oligomeric interfaces of OxyR, resulting in different relative rotation between the OxyR monomers. The domain rotation is likely to play a role in changing DNA binding of OxyR under reducing and oxidizing conditions[11]. A recent homology modeling study of full-length OxyR, which included both the DNA binding and regulatory domains, provides further evidence for a role of domain rotation in changing OxyR binding to DNA[13].

Despite the various biochemical and structural studies on OxyR summarized above, several key questions remain unanswered. What are the roles of the disulfide bond and intermediates during oxidation of OxyR? What are the forces driving the large structural switch during oxidation and reduction? We investigated the oxidation mechanism of OxyR in detail by a combination of mass spectrometry, UV-visible and fluorescence spectroscopy, and time-resolved kinetic analyses on C199S and C208S mutants as well as wild-type OxyR. These studies revealed that (i) a specific disulfide bond is formed between Cys199 and Cys208 upon wild-type OxyR reaction with H_2O_2; (ii) the transition to the oxidized form of OxyR is very fast, with a rate of 9.7 s^{-1}; and (iii) oxidized OxyR is conformationally strained, and this seems to be used as the driving force for the conformational change toward the reduced form. These results indicate that the specific disulfide bond–mediated structural switch of OxyR is based on kinetic and thermodynamic driving forces in oxidation and reduction steps, respectively.

[1]Center for Cellular Switch Protein Structure and [2]Systemic Proteomics Research Center, Korea Research Institute of Bioscience and Biotechnology, 52 Euh-eun-dong, Yuseong-gu, Daejeon 305-806, Korea. [3]Life Sciences Division and [4]Functional Proteomics Center, Korea Institute of Science and Technology, PO Box 131, Cheongryang, Seoul 130-650, Korea. [5]Cell Biology and Metabolism Branch, National Institute of Child Health and Human Development, National Institutes of Health, Bethesda, Maryland 20892, USA. Correspondence should be addressed to S.E.R. (ryuse@kribb.re.kr).

Published online 14 November 2004; doi:10.1038/nsmb856

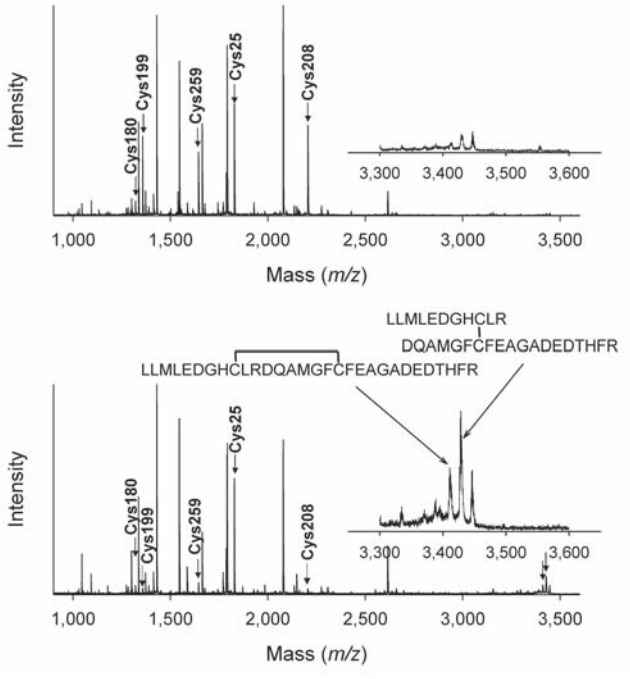

Figure 1 MALDI-TOF spectra for the tryptic digests of reduced (top) and oxidized (bottom) wild-type OxyR. His_6-tagged wild-type OxyR protein was incubated in 100 mM DTT for 1 h and desalted by gel filtration chromatography before alkylation and digestion. To prepare oxidized OxyR, reduced protein was treated with eight equivalents of H_2O_2 at room temperature for 5 min before alkylation. Peptides containing IA-modified cysteines were marked by arrows and labeled according to the residue number of the cysteine.

RESULTS

Disulfide bond formation in purified protein

A recent study[12] questioning the notion that oxidation of OxyR results in the formation of a redox-active disulfide bond led us to re-examine the status of the cysteine residues in wild-type full-length OxyR. In this study, the Cys180-Cys259 disulfide bond was detected[12] instead of the previously proposed redox-active Cys199-Cys208 bond[4,9–10]. The analyses used air-oxidized OxyR purified from *E. coli*. We speculated that the air-oxidized OxyR might contain non-natural cysteine derivatives including mismatched disulfide bonds owing to incorrect folding or disulfide bond rearrangement during the extended periods of purification and storage. Thus, we completely reduced wild-type full-length OxyR; the purified protein was treated with 100 mM DTT before iodoacetamide (IA) alkylation and mass spectrometry analysis.

There are six cysteines in wild-type full-length OxyR. In reduced OxyR, five peptides containing IA-modified cysteines were detected. They correspond to Cys25, Cys180, Cys199, Cys208 and Cys259 (**Fig. 1**). In oxidized OxyR, we observed similar peaks corresponding to IA-modified Cys25 and Cys180 peptides, whereas the peaks corresponding to fragments containing IA-modified Cys199 and Cys208 were greatly reduced and the peak containing IA-modified Cys259 was reduced several-fold. Among the six cysteines in OxyR, we did not detect the peptide containing IA-modified Cys143 (IA-Cys143) in either reduced or oxidized OxyR. In the crystal structures of reduced and oxidized OxyR, the side chain of Cys143 (mutated to alanine in the structures) is completely buried[11]. The solvent-inaccessibility of Cys143 may have prohibited the residue from the IA modification that was carried out under nondenaturing conditions (see Methods). Consistent with this observation, Kim *et al.* also reported that Cys143 could only be modified only after the protein was denatured[12].

For the oxidized protein, we detected a peak that corresponds to the sum of the Cys199- and Cys208-containing peptide fragments joined by a disulfide bond in conjunction with two more peaks (**Fig. 1**). One peak at $m/z = 3{,}425.5$ was 18 Da smaller than the peak at $m/z = 3{,}443.5$, and must have arisen owing to the reduced accessibility of the cleavage site at position 201. The other, at $m/z = 3{,}459.5$, was 16 Da bigger, presumably owing to methionine sulfoxidation. All three peaks disappeared when the tryptic digests were treated with 20 mM DTT, and as expected, the peak at $m/z = 3{,}425.5$ gained 2 units (data not shown). Therefore, all three peaks correspond to peptides with disulfide bonds between Cys199 and Cys208. These data indicate that Cys199 and Cys208 form a disulfide bond when wild-type OxyR is oxidized by H_2O_2. Our clear evidence for a disulfide bond between Cys199 and Cys208 disulfide bond in oxidized wild-type OxyR is in disagreement with the data of Kim *et al*[12]. This discrepancy may be due to differences in the sample preparation method as described above.

Disulfide bond formation in *E. coli* cells

To test whether disulfide bond formation occurs between Cys199 and Cys208 in wild-type full-length OxyR *in vivo*, we examined the ability of different cysteine mutant derivatives to be alkylated by 4-acetamido-4′-maleimidylstilbene-2,2′-disulfonic acid (AMS) before and after cells were treated with 1 mM H_2O_2. The difference in the mobility of the wild-type and single-mutant OxyR in H_2O_2-untreated cells provides a measure of band separation by 500-Da AMS modification (**Fig. 2**). The 1,000-Da difference of wild-type OxyR between untreated and treated cells is consistent with the formation of a single disulfide bond. Three cysteine mutants, C25S, C143S and C259S, showed a similar 1,000-Da difference in mobility consistent with the formation of a single disulfide bond upon exposure to H_2O_2. A small amount of the remaining reduced form for the C25S mutant treated with H_2O_2 is probably due to the elevated expression of this derivative, which carries a mutation in the DNA-binding domain and cannot autoregulate its own expression. The oxidized form of C180S showed faster migration than the other mutants. We suggest that this is due to an altered conformation or the formation of a second disulfide bond. In contrast to the other mutants, there was no difference in mobility in the C199S and C208S derivatives from untreated and H_2O_2-treated cells. These results support the conclusion that the only disulfide bond formed in the wild-type protein in cells exposed to H_2O_2 is a disulfide bond between Cys199 and Cys208.

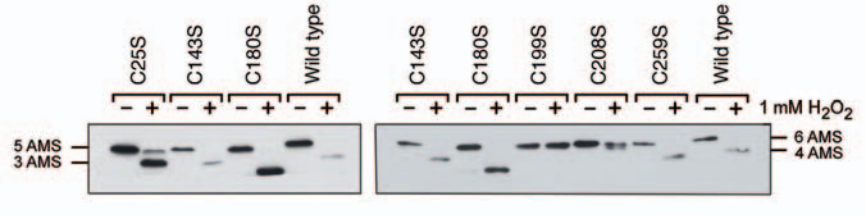

Figure 2 AMS analysis of OxyR cysteines in cells treated with H_2O_2. A strain carrying an *oxyR* deletion on the chromosome (TA4112) was transformed with plasmids expressing wild-type OxyR or OxyR derivatives in which each of the six cysteines was individually mutated to serine. The alkylated proteins were separated by nonreducing SDS-PAGE, transferred to nitrocellulose membranes and probed with OxyR-specific antiserum. OxyR modified by 3, 4, 5 or 6 AMS moieties has the indicated mobilities.

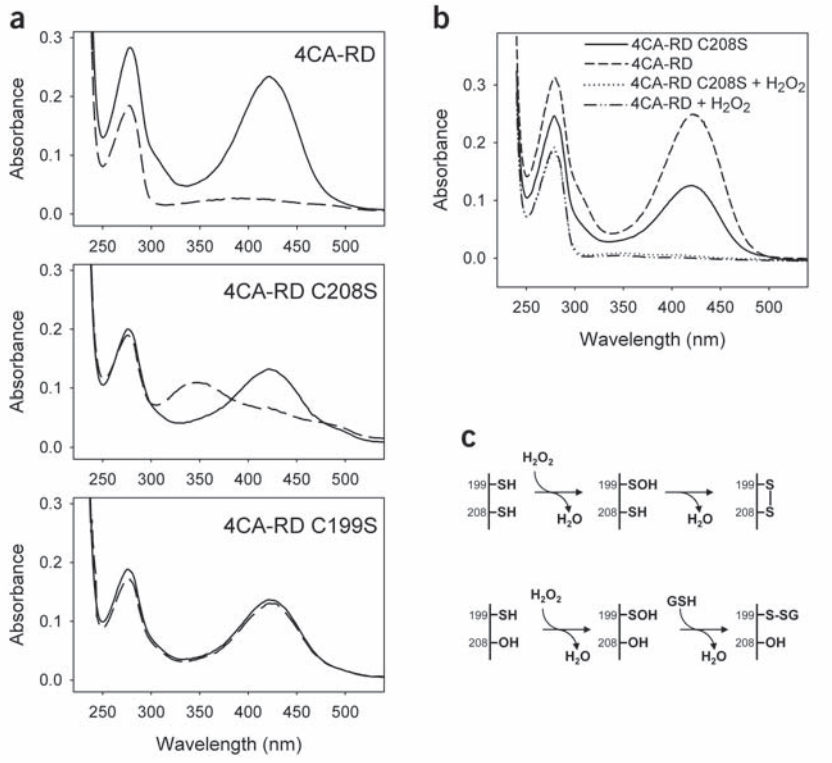

Figure 3 Characterization of OxyR oxidation by chemical modification. (**a**) UV-visible spectra of OxyR modified by 7-chloro-4-nitrobenzo-2-oxa-1,3-diazole (NBD-Cl). OxyR 4CA-RD, 4CA-RD C208S and 4CA-RD C199S were treated with NBD-Cl, and the residual reagent was removed on Sephadex G-25. UV-visible spectrum of each sample was recorded in a buffer containing 5 M guanidine. Analysis of oxidized protein, pretreated with two equivalents of H_2O_2, was done under similar conditions. Spectra of reduced and oxidized samples are solid and broken lines, respectively. (**b**) Effects of free surrounding thiols on OxyR oxidation. Samples were prepared as in **a** except that the sample buffer contained 0.5 mM GSH. (**c**) Proposed reaction scheme of OxyR oxidation by H_2O_2. Sulfhydryl (for cysteine) and hydroxyl (for serine) groups are denoted as SH and OH, respectively.

Oxidation through a two-step mechanism

To understand the mechanism of disulfide bond formation between Cys199 and Cys208, we carried out UV-visible spectroscopy analysis using the regulatory domain (RD, residues 81–305) of the OxyR mutant in which all cysteines except Cys199 and Cys208 are replaced with alanines (4CA-RD). The 4CA-RD mutant and two derivatives (4CA-RD C208S and 4CA-RD C199S) were treated with excess 7-chloro-4-nitrobenzo-2-oxa-1,3-diazole (NBD-Cl) with or without the prior exposure to two equivalents of H_2O_2. The NBD treatment of reduced 4CA-RD resulted in a new absorbance maximum at 420 nm (**Fig. 3a**) that corresponded to the spectrum of the previously characterized thiol adduct with NBD-Cl[14]. Quantification of this NBD-thiol adduct using molar extinction coefficient of 13,000 M^{-1} cm^{-1} indicated that ~90% of both cysteines were modified by NBD-Cl. H_2O_2-oxidized 4CA-RD, however, had no absorption >320 nm (**Fig. 3a**), consistent with disulfide bond formation between Cys199 and Cys208 as shown in the wild-type full-length protein.

NBD modification of reduced 4CA-RD C208S showed the same spectral species as reduced 4CA-RD. The absorption intensity at 420 nm was reduced because 4CA-RD C208S has only one cysteine, at residue 199. Oxidized 4CA-RD C208S, on the other hand, gave a different NBD-modified product with absorption maximum at 345 nm (**Fig. 3a**). This spectral signature is characteristic for NBD-sulfenate ester or sulfoxide form[14]. Hence, we conclude that oxidation of Cys199 by H_2O_2 generates cysteine sulfenic acid. NBD modification of reduced and oxidized 4CA-RD C199S showed similar spectra to that of NBD thioester (absorption peak at 420 nm), indicating that Cys208 is resistant to oxidation by H_2O_2.

Sulfenic acids are usually very unstable and readily react with accessible thiols to form a disulfide bond, releasing one molecule of water[15]. We speculate that the detection of sulfenic acid in 4CA-RD C208S was due to the lack of partner thiol. Therefore, we also investigated the oxidation of 4CA-RD and 4CA-RD C208S in the presence of 0.5 mM glutathione (GSH). GSH had little effect on the spectra of either reduced or oxidized 4CA-RD (**Fig. 3b**). In comparison, the UV-visible spectrum of NBD-Cl-treated oxidized 4CA-RD C208S changed considerably upon GSH addition. In contrast to our findings for the oxidized product in the absence of GSH, we did not find any spectral signature for sulfenic acid or free thiol (**Fig. 3b**). From these observations we conclude that oxidation of OxyR by H_2O_2 proceeds in a two-step mechanism that involves selective oxidation of Cys199 to form sulfenic acid and its subsequent reaction with Cys208, resulting in an intramolecular disulfide bond (**Fig. 3c**). The reaction between

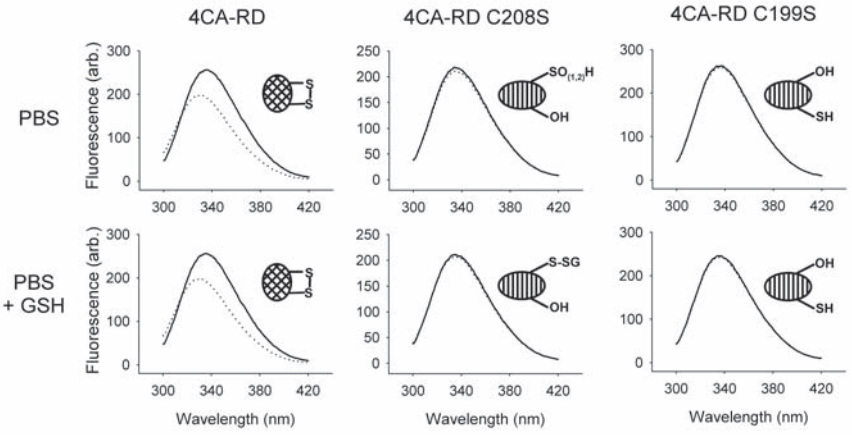

Figure 4 Steady-state fluorescence spectra of OxyR. Spectra were obtained for OxyR 4CA-RD, 4CA-RD C208S and 4CA-RD C199S in PBS containing 1 mM EDTA (top), or the same buffer containing 5 mM GSH (bottom). Emission spectra were scanned from 300 to 420 nm with excitation at 280 nm before (solid line) and after (dotted line) the addition of H_2O_2. Cartoons represent plausible reaction product under each experimental condition.

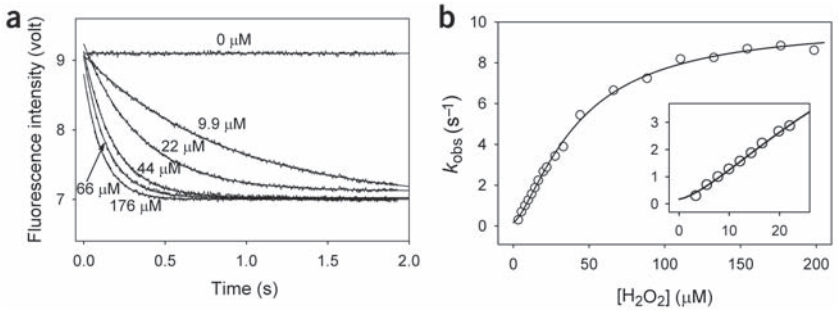

Figure 5 Stopped-flow measurement of conformational switch of OxyR during oxidation. (**a**) Kinetic traces of the pseudo-first-order reaction of OxyR. Experiments were carried out in PBS containing 1 mM EDTA at 25 °C at a final concentration of 0.94 μM reduced OxyR 4CA-RD and the indicated concentrations of H_2O_2. (**b**) The observed rate constants plotted against the concentration of H_2O_2. The line represents a sigmoidal Hill plot fitted to the data. Inset, the fitting in the region of low H_2O_2 concentrations.

Cys199 sulfenic acid (Cys199–SOH) and Cys208 should be very fast as there is no observed reaction of Cys199–SOH with surrounding GSH if Cys208 is present.

Intrinsic tryptophan fluorescence

Disulfide bond formation in OxyR results in a substantial structural change in the regulatory domain. We monitored the redox-related structural change by fluorescence spectroscopy. Oxidation of 4CA-RD by H_2O_2 resulted in a blue shift of the emission spectrum from 336 to 332 nm. In addition, the fluorescence intensity decreased by ~20% (**Fig. 4**). Because such a blue shift and decrease in quantum yield occurred irrespective of the excitation wavelength and in the range of tryptophan's characteristic emission spectra, the result indicates that the fluorescence change is mainly dependent on the local environment of the unique tryptophan (residue 175).

Trp175 is located in the center of the C-terminal domain of OxyR regulatory domain close to the region of structural changes upon oxidation[11]. Among the oxidation-mediated structural changes, it is notable that His198 moves close to Trp175 upon oxidation (from 22 Å in reduced form to 13 Å in oxidized form). Moreover, residues 210–215, which show high flexibility in the reduced form, are greatly stabilized in the oxidized form. The region contains one aspartic acid and two glutamic acids with distances to Trp175 ranging from 9 to 13 Å. Because histidine, aspartic acid and glutamic acid residues are good fluorescence quenchers in the distances as great as ~10 Å (ref. 16), it is likely that movement of those residues toward Trp175 mainly accounts for the increased quenching of the tryptophan fluorescence during oxidation.

Notably, oxidation of 4CA-RD C208S did not yield a fluorescence change (**Fig. 4**). This indicates that fluorescence change observed during oxidation of 4CA-RD is due to disulfide bond formation and that oxidation of Cys199 is not sufficient for the fluorescence change. Oxidized Cys199 is likely to destabilize the Cys199-containing loop[11]. However, the loop destabilization would not affect the fluorescence because the above-mentioned structural motifs related to the Trp175 fluorescence quenching are not stabilized before disulfide bond formation. In the presence of 5 mM GSH also, only 4CA-RD, which has two intact cysteines, showed fluorescence change (**Fig. 4**). Together, these data all indicate that fluorescence change occurs when the intramolecular disulfide bond is formed and provide additional evidence for our previous observation that oxidation of OxyR by H_2O_2 induces an intramolecular disulfide bond even in the presence of surrounding free thiols.

Conformational switch rate

The large decrease in quantum yield of tryptophan fluorescence enabled us to measure the time-resolved structural change of OxyR (4CA-RD) upon oxidation. Our earlier data suggested that oxidation proceeds via a two-step mechanism that can be represented by $OxyR_{re} + H_2O_2 \rightarrow OxyR'$ (rate: k_1); $OxyR' \rightarrow OxyR_{ox}$ (rate: k_2). The change in tryptophan fluorescence was measured under pseudo-first-order reaction conditions where reduced OxyR was rapidly mixed with increasing amounts of H_2O_2 using a stopped-flow instrument (**Fig. 5a**). The plot of rate constants versus H_2O_2 concentrations showed slightly sigmoidal character, suggesting that the protein has some cooperative behavior (**Fig. 5b**). Thus, the data were fitted to the following Hill equation, $k_{obs} = (k_{obs})_{min} + (k_{obs})_{max}[H_2O_2]^n / (K_{1/2}{}^n + [H_2O_2]^n)$, where $(k_{obs})_{min}$ and $(k_{obs})_{max}$ are minimum and maximum rates of the conformational change, $K_{1/2}$ is the half saturation constant and n is the Hill coefficient[17]. The values

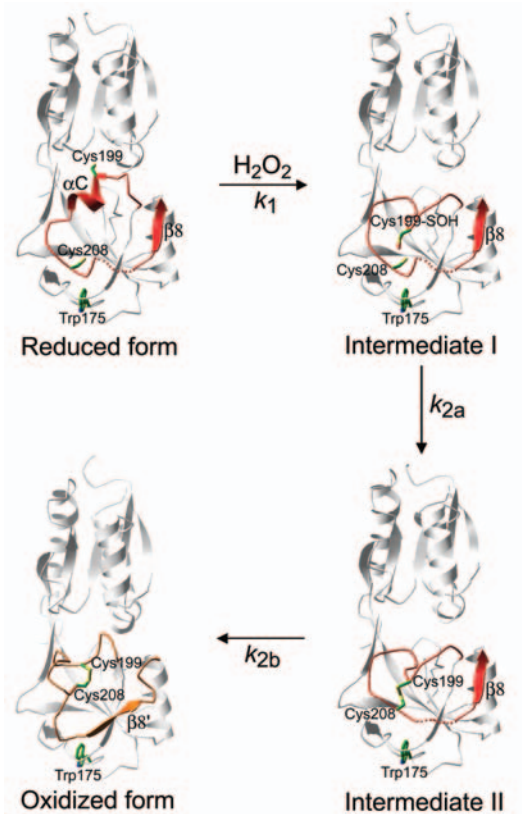

Figure 6 Intermediates in the structural transitions of OxyR. Presumptive intermediates during the oxidative structural transitions of OxyR are shown. Intermediate I: induced flexibility of the Cys199 region due to Cys199 oxidation. Intermediate II: disulfide bond formation between Cys199 and Cys208 before structural rearrangement in C-terminal domain. The region playing an important role in the structural transition (residues 195–223 including αC and β8) is red. Residues 211–216 were not identified in the reduced-form structure[11] and are small dots in the figure. In the oxidized form, the 195–223 region is gold.

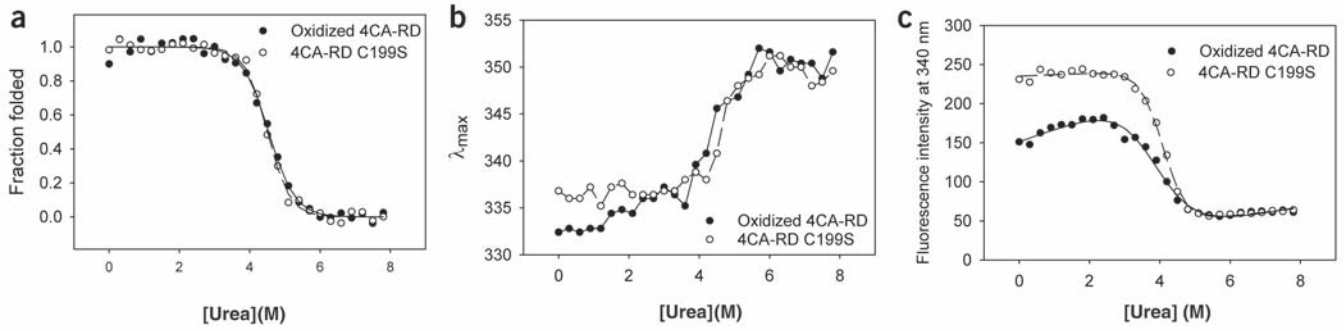

Figure 7 Urea-induced equilibrium unfolding transition of OxyR. (**a**) Equilibrium unfolding of OxyR 4CA-RD C199S and oxidized OxyR 4CA-RD was monitored by CD spectroscopy. Molar ellipticity then was measured at 222 nm. Symbols are experimental data, and lines are fitted curves. (**b**,**c**) Equilibrium unfolding was monitored by fluorescence spectroscopy. The data for λ_{max} and emission at 340 nm were extracted and plotted. Symbols and lines are the same as in **a**.

for the Hill coefficient, $K_{1/2}$, $(k_{obs})_{max}$ and $(k_{obs})_{min}$ were determined to be 1.4 ± 0.1, 43 ± 2 μM, 9.7 ± 0.4 s^{-1} and 0.18 ± 0.15 s^{-1}, respectively. The positive Hill coefficient is consistent with the observation of dimers in the OxyR crystal structure. The dimeric contacts of reduced OxyR are switched upon oxidation, leading to intermonomer rotation in the oxidized OxyR dimer[11]. It seems that the oxidative structural switch in one monomer facilitates the same changes in the next monomer through structural changes at the dimeric interfaces.

The maximum rate $(k_{obs})_{max}$, which can be approximated to k_2, is similar to that of ATP-induced allosteric transition in eukaryotic chaperonin CCT (two phases of 10 s^{-1} and 17 s^{-1})[18] and lies in the range of folding rate constants of some small proteins that fold via a two-state mechanism[19]. The minimum rate $(k_{obs})_{min}$ is close to zero, suggesting that conformational change does not occur without prior oxidation by H_2O_2 (refs. 17,18). Based on the fitted curve, the rate of conformation change at 43 μM of H_2O_2 is 4.9 s^{-1}. The values allow the estimation of the lower limit of the association rate (k_1) between reduced OxyR and H_2O_2 to be 1.1×10^5 M^{-1} s^{-1}, quite close to the rate of ~10^7 M^{-1} min^{-1} determined by differential cysteine modification followed by SDS-PAGE analysis[9].

The conformational change should consist of more than one chemical step including disulfide bond formation (k_{2a}) as well as the physical step of conformation change (k_{2b}) (**Fig. 6**). Currently, we do not know which subreaction corresponds to the rate of 9.7 s^{-1}. Assuming that Cys208 competes with GSH in the reaction with Cys199-SOH and the association rate of GSH lies in the range of 10^5 10^6 M^{-1} s^{-1}, the rate we measured is unlikely to be the rate for the chemical reaction of Cys208 and Cys199-SOH. The molar concentration of GSH in the cell is ~5 mM, which would result in a first-order rate of two or three orders of magnitude higher than k_2. Therefore, we tentatively assign the measured rate as that of conformational switch (k_{2b}) after the much faster intramolecular disulfide bond formation (k_{2a}).

Destabilization by oxidation

To further understand the forces driving the redox-mediated conformation switch, we analyzed the conformation stability of reduced and oxidized OxyR by denaturant-induced equilibrium unfolding. We first examined the conformational stability by circular dichroism (CD) spectroscopy (**Fig. 7a**). Because of difficulty in maintaining reducing conditions during our measurements, we used 4CA-RD C199S instead of reduced 4CA-RD. As the denaturant concentration increased, ellipticity at 222 nm decreased. The unfolding profiles were almost identical for 4CA-RD C199S and oxidized 4CA-RD, suggesting that overall stability is not perturbed by the formation of the disulfide bond. The CD data showed a single unfolding transition at 4.5 M urea.

Next, we applied fluorescence spectroscopy to monitor unfolding (**Fig. 7b**,**c**). Incubation of the proteins in 8 M urea resulted in the emission maxima (λ_{max}) becoming red-shifted to 350 nm with decreased overall intensity. Between 3.5 and 5.5 M urea, λ_{max} increased, indicating an increase in solvent exposure of the tryptophan residue as the proteins unfolded (**Fig. 7b**). Even though we could not analyze the λ_{max} data further due to high uncertainty, it is clear that the transition occurs later than the quenching of tryptophan fluorescence (monitored in **Fig. 7c**). The fluorescence emission intensity data of OxyR (**Fig. 7c**) were fitted to a two-state unfolding model to give the $D_{1/2}$ (transition midpoint) and *m*-value (constant of proportionality between denaturant concentration and free energy of unfolding) as shown in **Table 1**. There were significant differences in both the $D_{1/2}$ and *m*-value of the proteins. $D_{1/2}$ for oxidized 4CA-RD was 3.8 M, which is 0.3 M lower than $D_{1/2}$ for 4CA-RD C199S. The *m*-value was also lower. The ΔG_{H_2O} calculated using $D_{1/2}$ and *m*-value indicates that the conformation of the oxidized state is destabilized by ~3 kcal mol^{-1} compared with that of 4CA-RD C199S. Though a long extrapolation was used for the determination of ΔG_{H_2O} for 4CA-RD C199S, this form of OxyR is certainly more stable than oxidized 4CA-RD as the value of transition midpoint also is higher.

DISCUSSION

Reversible disulfide bond formation and associated conformation changes are likely to play an important role in cellular redox regulation. In particular, disulfide bond formation between distant cysteines could be an effective mechanism to induce conformational changes that lead to switches in protein activity[11,20]. The results presented here clearly show that a specific disulfide bond is formed between Cys199 and Cys208 in the redox-regulated OxyR protein exposed to oxidative stress. The oxidation-induced disulfide bond formation and consequent structural switches occur with fast reaction kinetics, and the structural destabilization of the oxidized form seems to drive the reverse reaction upon reduction of the disulfide bond.

Previously, Kim *et al.* proposed that Cys180 and Cys259 could form a disulfide bond[12]. However, we did not detect a peptide containing a disulfide bond between Cys259 and any other cysteine-containing peptides. Thus, the decreased peak intensity of IA-Cys259 (**Fig. 1**) may be due to the structural difference between reduced and oxidized OxyR in the region[11], although possibilities for the disulfide bond formation cannot be excluded. In either case, the modification of Cys259 is unlikely to play a major role in the function of OxyR, because Cys180 and Cys259 are not critical to the transcriptional activity of OxyR[6]. Another notable discrepancy between our findings and the data of Kim *et al.* is that we were able to detect IA-Cys208 in reduced OxyR,

Table 1 Thermodynamic parameters of OxyR

Protein	$D_{1/2}$ (M)	m (kcal mol^{-1} M^{-1})	ΔG_{H_2O} (kcal mol^{-1})
Fluorescence (340 nm)			
4CA-RD (oxidized)	3.8	1.1	4.2
4CA-RD C199S	4.1	1.8	7.4
Circular dichroism (222 nm)			
4CA-RD (oxidized)	4.5	1.6	7.2
4CA-RD C199S	4.5	1.8	8.1

whereas Kim *et al.* could not detect this peptide. In the crystal structure of reduced OxyR[11], Cys208 is partially exposed to solvent and likely to be modified by IA in its native state. The air-oxidized OxyR used by Kim *et al.* may have contained an inadvertently oxidized Cys208, prohibiting its IA modification.

The formation of a specific Cys199-Cys208 disulfide bond is consistent with previous reports that the C199S and C208S mutations both disrupt induction of *oxyS*, a prominent OxyR target gene[4]. However, the C208S mutant was less sensitive to H_2O_2 than the C199S mutant in zone of inhibition assays[6], raising the question whether the disulfide bond formation is essential for the transcriptional activity of OxyR. To further examine the C208S activity, we constructed a C199S C208S double mutant and found that this mutant shows the same intermediate sensitivity as the C208S single mutant (see **Supplementary Table 1** online). The C208S mutation seems to render the OxyR slightly constitutively active such that the mutant protein activates transcription independent of oxidative stress. Consistent with these observations, a C208Y derivative was isolated as a constitutively active mutant in the previous random mutagenesis study[6]. We suggest that mutations at the Cys208 position change local structure and allow some interaction between OxyR and RNA polymerase, resulting in gene activation. For the wild-type protein, the interaction with RNA polymerase and activation requires that the oxidized conformation of OxyR be stabilized by the Cys199-Cys208 disulfide bond.

In the crystal structure of reduced OxyR[11], Cys199 and Cys208 are separated by 17 Å, too far apart to form a disulfide bond. Oxidation of Cys199 into the sulfenic acid (SOH) results in destabilization of the Cys199 side chain in the hydrophobic binding pocket owing to its increased size and charge[11]. The destabilization is likely to lead to expulsion of the side chain of Cys199 out of the interdomain pocket, resulting in a flexible loop around Cys199 (**Fig. 6**). The crystal structure also indicated flexibility in the 205–216 region, which contains Cys208 in the middle. Flexibility of both the Cys208 and the Cys199 regions should increase chances for collision between Cys199-SOH and Cys208, and disulfide bond formation between them (k_{2a}). After the disulfide bond is formed, the flexible regions start to reorganize into the new conformation (k_{2b}), which involves translocation of strand β8 to β8′ and adjustment of residues in the region near Trp175, leading to the fluorescence change in the oxidized form. However, further studies are needed for full validation of this hypothetical model.

The nonsuperimposable unfolding transitions observed with different spectroscopic probes (CD and fluorescence) imply an unfolding intermediate of OxyR. The transition measured by fluorescence intensity probably corresponds to the local unfolding of the tertiary structure and the transition monitored by CD probably corresponds to the global unfolding of the intermediate. The local unfolding is most likely to occur in the region of the disulfide bond–mediated structural switch that is near Trp175. The intermediate structure seems to have some of the attributes of molten globule[21]: the tertiary structure is disturbed, as shown by the lower fluorescence intensity, but the secondary structure is still largely intact, as indicated by the strong α-helix signal in CD. A similar phenomenon has been reported for the case of bacterial protein FtsZ, in which local unfolding precedes global unfolding[22]. Preferential loss of functional properties of FtsZ occurred at lower urea concentrations than global unfolding as measured by CD[22].

In the transcription initiation complex, OxyR binds to RNA polymerase and DNA. These interactions stabilize the oxidized form of OxyR[6], indicating that the conformational strain of oxidized OxyR could be compensated by the intermolecular interaction energy in the ternary complex involving OxyR, RNA polymerase and DNA. After the transcription initiation, OxyR dissociated from the complex is likely to favor the reduced conformation, especially when the intracellular environment has returned to the normal reduced state. Metastability has been known to be essential for functional regulation of some proteins such as serine protease inhibitors and the membrane fusion protein of influenza virus, in which the strain loaded on the native structures drives conformational rearrangement during functional execution[23,24]. OxyR seems to be one more example in which metastability controls biological activity.

METHODS

Purification of OxyR protein. The gene for wild-type full-length OxyR was cloned into NdeI-HindIII restriction sites of pET-28a vector (Novagen), and the N-terminal His_6-tagged OxyR protein was expressed from *E. coli* BL21(DE3) at 18 °C . The OxyR regulatory domain (RD, residues 81–305) in which all cysteines except for Cys199 and Cys208 were replaced with alanines, was subcloned into pET-21a vector; we designate this as 4CA-RD. Two more mutants (4CA-RD C208S and 4CA-RD C199S) were constructed from 4CA-RD by using the QuikChange site-directed mutagenesis kit (Stratagene) and confirmed by DNA sequencing. The 4CA-RD proteins expressed from *E. coli* BL21(DE3) at 20 °C were purified as described[11]. OxyR was reduced by incubating the purified protein in 100 mM DTT for 1 h and desalted using Sephadex G-25 on an AKTA FPLC system (Amersham-Pharmacia Biotech). All buffers used in the desalting procedure were prepared freshly before use and completely degassed.

Mass spectrometry. Wild-type OxyR protein (200 µl of 0.1 mg ml^{-1}, 2.7 µM) in a buffer of 20 mM Tris, pH 7.4, 0.3 M KCl, 5 mM $MgCl_2$, 0.5 mM EDTA, and 10% (v/v) glycerol was treated with 20 mM iodoacetamide (Sigma) in the dark at room temperature for 1.5 h. The sample was exhaustibly dialyzed against 10 mM Tris, pH 7.4, and incubated with trypsin (2 µl of 0.5 mg ml^{-1}, Sigma) overnight at 37 °C to digest the alkylated protein. Subsequently, 1/100 volume of 10% (v/v) TFA was added to stop the reaction. MALDI-TOF mass spectra were obtained on a Voyger-DE STR MALDI-TOF mass spectrometer (Applied Biosystems). For the analysis of oxidized OxyR, the protein was treated with eight equivalents of H_2O_2 (22 µM) at room temperature for 5 min before alkylation.

***In vivo* disulfide bond determination assay.** Cells were grown aerobically to exponential phase (A_{600} = 0.4-0.6) in LB medium at 37 °C. Aliquots of the cultures (1 ml) then were transferred into an anaerobic chamber (Coy Laboratories). Half of the culture was left untreated and the other half was exposed to 1 mM H_2O_2. The 1 mM H_2O_2 treatment was necessary to obtain consistent oxidation of the proteins expressed from the multicopy pUC18 vector. After 5 min, the cells were mixed with 50 µl ice-cold 100% (w/v) TCA and collected immediately. The pellets were dissolved in freshly prepared AMS buffer (15 mM AMS, 1 M Tris, pH 8.0, 0.1% (w/v) SDS) and incubated at 37 °C for 1 h. The samples then were mixed with 3× Red loading buffer (New England Biolabs) without DTT. After electrophoresis, the proteins were transferred to a Protran nitrocellulose membrane (Schleicher and Schuell) and probed with polyclonal rabbit antiserum against OxyR. The bound antibodies were detected using the Supersignal West Pico Chemiluminescent kit (Pierce).

Modification of OxyR with 7-chloro-4-nitrobenzo-2-oxa-1,3-diazole. OxyR 4CA-RD (750 µl of 0.4 mg ml^{-1}, 16 µM) in PBS containing 1 mM EDTA was treated with 24 µl of 20 mM NBD-Cl (Aldrich) at room temperature for

2 h. Residual reagent was removed by desalting using Sephadex G-25. The protein samples were then concentrated to 240 µl and mixed with 360 µl of 8.4 M guanidine hydrochloride to completely unfold OxyR protein. For analysis of the oxidized protein, the same procedure was followed except that samples were treated with two equivalents of H_2O_2 (32 µM) for 5 min before modification with NBD-Cl. UV-visible spectra were recorded on a Beckman spectrophotometer.

Steady-state fluorescence spectroscopy. Fluorescence spectroscopy was carried out in PBS containing 1 mM EDTA at 25 °C on an RF-5000 spectrofluorometer (Shimazu). Fluorescence emission spectra of 4CA-RD were recorded from 300 to 420 nm with excitation at both 280 and 293 nm. Steady-state fluorescence data for 25 µg OxyR 4CA-RD protein per 2.5 ml solution were obtained at 25 °C using a 1 × 1 cm cuvette. To monitor fluorescence change upon reaction with H_2O_2, 10 µl of 2.5 mM H_2O_2 was added to the protein solution and the fluorescence was scanned again. All spectra were corrected for background and adjusted for dilution caused by the addition of H_2O_2.

Stopped-flow experiment. Time-resolved fluorescence change was measured with an SFM-4 stopped-flow apparatus (Bio-Logic). Experiments were carried out in PBS containing 1 mM EDTA at 25 °C at a final concentration of 0.94 µM of reduced OxyR 4CA-RD and various concentrations of H_2O_2. For the reliable concentrations of H_2O_2, a stock solution of 50 mM H_2O_2 was prepared from a commercially available 30% (w/w) H_2O_2 solution (Fisher) by dilution with the buffer. The stock solution was maintained on ice, diluted appropriately and used on the same day. Intrinsic tryptophan was excited at 280 nm, and the change in fluorescence >320 nm was measured by using a 320-nm cutoff filter. Stopped-flow traces were analyzed by fitting to a single-exponential function ($y = y_0 + A \exp(-k_{obs}t)$). The observed rate constants (k_{obs}) were then plotted as a function of [H_2O_2], and the data were fitted to a Hill equation[17]. All fitting procedures were done using nonlinear regression tools of SigmaPlot software from Jandel Scientific.

Equilibrium unfolding. Equilibrium unfolding by CD spectroscopy was carried out as a function of urea. Fresh urea solutions were made in PBS buffer and used for each unfolding experiment. OxyR 4CA-RD (0.15 mg ml^{-1}) was equilibrated in various concentrations of urea at 25 °C for 5 h. For each sample, ellipticity at 222 nm was measured. Fluorescence spectroscopy was also applied for the equilibrium unfolding study. In this case, 10 µg ml^{-1} of OxyR 4CA-RD protein was used in PBS containing 1 mM EDTA, and emission spectrum was scanned from 300 to 420 nm with excitation at 280 nm. The data were fitted to a two-state unfolding equation using SigmaPlot software, which gave us $D_{1/2}$ (the denaturant concentration at which the protein is half unfolded) and *m*-value (proportionality constant of the free energy to denaturant concentration)[25]. The free energy of unfolding at 0 M denaturant is given by the product of the two values ($\Delta G_{H2O} = D_{1/2} \times m$).

Note: Supplementary information is available on the Nature Structural & Molecular Biology website.

ACKNOWLEDGMENTS
We thank A. Matouschek for helpful suggestions on the equilibrium unfolding study, and W. Outten for comments on the manuscript. This research was supported by the National Creative Research Initiative Program (MOST, Korea) and the Korea Research Institute of Bioscience and Biotechnology Research Initiative Program.

COMPETING INTERESTS STATEMENT
The authors declare that they have no competing financial interests.

Received 16 July; accepted 7 October 2004
Published online at http://www.nature.com/nsmb/

1. Halliwell, B. & Gutteridge, J.M.C. *Free Radicals in Biology and Medicine* Oxford University Press, New York (1999).
2. Lander, H.M. An essential role for free radicals and derived species in signal transduction. *FASEB J.* **11**, 118–124 (1997).
3. Storz, G., Tartaglia, L.A. & Ames, B.N. Transcriptional regulator of oxidative stress-inducible genes: direct activation by oxidation. *Science* **248**, 189–194 (1990).
4. Zheng, M., Aslund, F. & Storz, G. Activation of the OxyR transcription factor by reversible disulfide bond formation. *Science* **279**, 1718–1721 (1998).
5. Hausladen, A. *et al.* Nitrosative stress: activation of the transcription factor OxyR. *Cell* **86**, 719–729 (1996).
6. Kullik, I., Toledano, M.B., Tartaglia, L.A. & Storz, G. Mutational analysis of the redox-sensitive transcriptional regulator OxyR: regions important for oxidation and transcriptional activation. *J. Bacteriol.* **177**, 1275–1284 (1995).
7. Tao, K., Fujita, N. & Ishihama, A. Involvement of the RNA polymerase alpha subunit C-terminal region in co-operative interaction and transcriptional activation with OxyR protein. *Mol. Microbiol.* **7**, 859–864 (1993).
8. Toledano, M.B. *et al.*. Redox-dependent shift of OxyR-DNA contacts along an extended DNA-binding site: a mechanism for differential promoter selection. *Cell* **78**, 897–909 (1994).
9. Aslund, F., Zheng, M., Beckwith, J. & Storz, G. Regulation of the OxyR transcription factor by hydrogen peroxide and the cellular thiol-disulfide status. *Proc. Natl. Acad. Sci. USA* **96**, 6161–6165 (1999).
10. Tao, K. In vivo oxidation-reduction kinetics of OxyR, the transcriptional activator for an oxidative stress-inducible regulon in *Escherichia coli*. *FEBS Lett.* **457**, 90–92 (1999).
11. Choi, H. *et al.* Structural basis of the redox switch in the OxyR transcription factor. *Cell* **105**, 103–113 (2001).
12. Kim, S.O. *et al.* OxyR: a molecular code for redox-related signaling. *Cell* **109**, 383–396 (2002).
13. Zaim, J. & Kierzek, A.M. The structure of full-length LysR-type transcriptional regulators. Modeling of the full-length OxyR transcription factor dimer. *Nucleic Acids Res.* **31**, 1444–1454 (2003).
14. Ellis, H.R. & Poole, L.B. Novel application of 7-chloro-4-nitrobenzo-2-oxa-1,3-diazole to identify cysteine sulfenic acid in the AhpC component of alkyl hydroperoxide reductase. *Biochemistry* **36**, 15013–15018 (1997).
15. Claiborne, A. *et al.* Protein-sulfenic acids: diverse roles for an unlikely player in enzyme catalysis and redox regulation. *Biochemistry* **38**, 15407–15416 (1999).
16. Chen, Y., & Barkley, M.D. Toward understanding tryptophan fluorescence in proteins. *Biochemistry* **37**, 9976–9982 (1998).
17. Li, S., Rosen, B.P., Borges-Walmsley, M.I., & Walmsley, A.R. Evidence for cooperativity between the four binding sites of dimeric ArsD, an As(III)-responsive transcriptional regulator. *J. Biol. Chem.* **277**, 25992–26002 (2003).
18. Kafri, G. & Horovitz, A. Transient kinetic analysis of ATP-induced allosteric transitions in the eukaryotic chaperonin containing TCP-1. *J. Mol. Biol.* **326**, 981–987 (2003).
19. Grantcharova, V., Alm E.J., Baker, D., & Horwich, A.L. Mechanisms of protein folding. *Curr. Opin. Struct. Biol.* **11**, 70–82 (2001).
20. Georgiou, G. How to flip the (redox) switch. *Cell* **111**, 607–610 (2002).
21. Ptitsyn, O.B. Molten globule and protein folding. *Adv. Protein Chem.* **47**, 83–229 (1995).
22. Santra, M.K. and Panda, D. Detection of an intermediate during unfolding of bacterial cell division protein FtsZ. *J. Biol. Chem.* **278**, 21336–21343 (2003).
23. Carr, C.M. & Kim, P.S. A spring-loaded mechanism for the conformational change of influenza hemagglutinin. *Cell* **73**, 823–832 (1993).
24. Lee, C., Park, S.H., Lee, M.Y. & Yu, M.H. Regulation of protein function by native metastability. *Proc. Natl. Acad. Sci. USA* **97**, 7727–7731 (2000).
25. Fersht, A. In *Structure and Mechanism in Protein Science* (Freeman, New York, 1998).